

RESEARCH LETTER

10.1029/2018GL077728

Key Points:

- Large model overestimates of NO/NO<sub>2</sub> concentration ratios in the upper troposphere imply errors in NO-NO<sub>2</sub>-O<sub>3</sub> cycling kinetics or the presence of an unaccounted labile NO<sub>x</sub> reservoir
- The presence of an unaccounted labile NO<sub>x</sub> reservoir would affect the NO<sub>x</sub> lifetime in the upper troposphere and would suggest unrecognized, likely organic, chemistry
- Possible error in NO-NO<sub>2</sub>-O<sub>3</sub> cycling kinetics would have large implications for global simulations of tropospheric ozone and for satellite retrievals of tropospheric NO<sub>2</sub>

Correspondence to:

R. F. Silvern,  
rsilvern@harvard.edu

Citation:

Silvern, R. F., Jacob, D. J., Travis, K. R., Sherwen, T., Evans, M. J., Cohen, R. C., et al. (2018). Observed NO/NO<sub>2</sub> ratios in the upper troposphere imply errors in NO-NO<sub>2</sub>-O<sub>3</sub> cycling kinetics or an unaccounted NO<sub>x</sub> reservoir. *Geophysical Research Letters*, 45, 4466–4474. <https://doi.org/10.1029/2018GL077728>

Received 27 OCT 2017

Accepted 20 APR 2018

Accepted article online 30 APR 2018

Published online 12 MAY 2018

©2018. The Authors.

This is an open access article under the terms of the Creative Commons Attribution-NonCommercial-NoDerivs License, which permits use and distribution in any medium, provided the original work is properly cited, the use is non-commercial and no modifications or adaptations are made.

# Observed NO/NO<sub>2</sub> Ratios in the Upper Troposphere Imply Errors in NO-NO<sub>2</sub>-O<sub>3</sub> Cycling Kinetics or an Unaccounted NO<sub>x</sub> Reservoir

R. F. Silvern<sup>1</sup>, D. J. Jacob<sup>1,2</sup>, K. R. Travis<sup>3</sup>, T. Sherwen<sup>4,5</sup>, M. J. Evans<sup>4,5</sup>, R. C. Cohen<sup>6,7</sup>, J. L. Laughner<sup>6</sup>, S. R. Hall<sup>8</sup>, K. Ullmann<sup>8</sup>, J. D. Crouse<sup>9</sup>, P. O. Wennberg<sup>9,10</sup>, J. Peischl<sup>11,12</sup>, and I. B. Pollack<sup>13</sup>

<sup>1</sup>Department of Earth and Planetary Sciences, Harvard University, Cambridge, MA, USA, <sup>2</sup>John A. Paulson School of Engineering and Applied Sciences, Harvard University, Cambridge, MA, USA, <sup>3</sup>Department of Civil and Environmental Engineering, Massachusetts Institute of Technology, Cambridge, MA, USA, <sup>4</sup>Wolfson Atmospheric Chemistry Laboratories, Department of Chemistry, University of York, York, UK, <sup>5</sup>National Centre for Atmospheric Science, Department of Chemistry, University of York, York, UK, <sup>6</sup>Department of Chemistry, University of California, Berkeley, CA, USA, <sup>7</sup>Department of Earth and Planetary Science, University of California, Berkeley, CA, USA, <sup>8</sup>Atmospheric Chemistry Division, National Center for Atmospheric Research, Boulder, CO, USA, <sup>9</sup>Division of Geological and Planetary Sciences, California Institute of Technology, Pasadena, CA, USA, <sup>10</sup>Division of Engineering and Applied Science, California Institute of Technology, Pasadena, CA, USA, <sup>11</sup>Cooperative Institute for Research in Environmental Sciences, University of Colorado Boulder, Boulder, CO, USA, <sup>12</sup>Earth System Research Laboratory, National Oceanic and Atmospheric Administration, Boulder, CO, USA, <sup>13</sup>Department of Atmospheric Science, Colorado State University, Fort Collins, CO, USA

**Abstract** Observations from the SEAC<sup>4</sup>RS aircraft campaign over the southeast United States in August–September 2013 show NO/NO<sub>2</sub> concentration ratios in the upper troposphere that are approximately half of photochemical equilibrium values computed from Jet Propulsion Laboratory (JPL) kinetic data. One possible explanation is the presence of labile NO<sub>x</sub> reservoir species, presumably organic, decomposing thermally to NO<sub>2</sub> in the instrument. The NO<sub>2</sub> instrument corrects for this artifact from known labile HNO<sub>4</sub> and CH<sub>3</sub>O<sub>2</sub>NO<sub>2</sub> NO<sub>x</sub> reservoirs. To bridge the gap between measured and simulated NO<sub>2</sub>, additional unaccounted labile NO<sub>x</sub> reservoir species would have to be present at a mean concentration of ~40 ppt for the SEAC<sup>4</sup>RS conditions (compared with 197 ppt for NO<sub>x</sub>). An alternative explanation is error in the low-temperature rate constant for the NO + O<sub>3</sub> reaction (30% 1-σ uncertainty in JPL at 240 K) and/or in the spectroscopic data for NO<sub>2</sub> photolysis (20% 1-σ uncertainty). Resolving this discrepancy is important for understanding global budgets of tropospheric oxidants and for interpreting satellite observations of tropospheric NO<sub>2</sub> columns.

**Plain Language Summary** We identify large discrepancies between observed NO/NO<sub>2</sub> ratios and models representing our best understanding of the chemistry controlling NO and NO<sub>2</sub> in the upper troposphere over the southeast United States during August–September 2013. We suggest that either unrecognized chemistry or errors in modeled cycling between NO, NO<sub>2</sub>, and O<sub>3</sub> could explain this discrepancy. Either explanation will have important implications for global tropospheric chemistry and for the interpretation of satellite observations of NO<sub>2</sub>.

## 1. Introduction

Nitrogen oxide radicals (NO<sub>x</sub> ≡ NO + NO<sub>2</sub>) are emitted by anthropogenic sources (fuel combustion) and natural sources (lightning, soils, and fires). Anthropogenic emissions degrade surface air quality by producing ozone and nitrate particulate matter and also affect ecosystems through nitrogen deposition. On a global scale, NO<sub>x</sub> increases the concentration of tropospheric oxidants (ozone and OH) with complicated implications for climate forcing (Wild et al., 2001). NO<sub>x</sub> in the upper troposphere and the associated cycling between NO and NO<sub>2</sub> are of particular importance for production of tropospheric ozone and OH (Murray et al., 2013; Newsome & Evans, 2017; Ridley et al., 2017). Recent observations from the SEAC<sup>4</sup>RS aircraft campaign over the southeast United States in August–September 2013 show much lower NO/NO<sub>2</sub> ratios in the upper troposphere than expected from models (Travis et al., 2016). Here we suggest possible explanations for this discrepancy and discuss the implications for global tropospheric chemistry and for the interpretation of satellite NO<sub>2</sub> data.

The SEAC<sup>4</sup>RS observations over the southeast United States show NO<sub>x</sub> concentrations averaging 0.20 ppb in the upper troposphere above 8 km (0.11 ppb as NO and 0.09 ppb as NO<sub>2</sub>), as compared to 0.37 ppb in the boundary layer below 2 km (0.06 ppb NO and 0.31 ppb NO<sub>2</sub>), and much lower concentrations (averaging less than 0.07 ppb) in the middle troposphere between 2 and 8 km (Travis et al., 2016). Such a “C-shaped” profile reflects influences from fuel combustion in the boundary layer and lightning in the upper troposphere (Bertram et al., 2007; Hudman et al., 2007; Huntrieser et al., 2002; Pickering et al., 1998). The mean observed daytime NO/NO<sub>2</sub> ratios in SEAC<sup>4</sup>RS were 0.44 mol mol<sup>-1</sup> in the boundary layer and 1.4 mol mol<sup>-1</sup> in the upper troposphere, while the corresponding ratios in the GEOS-Chem chemical transport model sampled along the flight tracks were 0.33 mol mol<sup>-1</sup> in the boundary layer and 3.3 mol mol<sup>-1</sup> in the upper troposphere (Travis et al., 2016). The NO/NO<sub>2</sub> ratio in the model increases rapidly with altitude because of the strong temperature dependence of the NO + O<sub>3</sub> reaction (Burkholder et al., 2015), but in the observations this increase is much less.

NO<sub>2</sub> measurements in the upper troposphere are prone to positive interferences from inlet decomposition of thermally unstable compounds including HNO<sub>4</sub>, CH<sub>3</sub>O<sub>2</sub>NO<sub>2</sub>, and other organic nitrates (Bradshaw et al., 1999; Browne et al., 2011; Murphy et al., 2004; Nault et al., 2015; Reed et al., 2016). The Berkeley thermal-dissociation laser-induced fluorescence (TD-LIF) instrument used in SEAC<sup>4</sup>RS (Day et al., 2002; Thornton et al., 2000; Wooldridge et al., 2010) was specifically designed to minimize and correct for these interferences. Inlet residence time is only 0.23 s, and the NO<sub>2</sub> measurement is corrected for partial thermal dissociation of HNO<sub>4</sub> (0–11%) and CH<sub>3</sub>O<sub>2</sub>NO<sub>2</sub> (0–21%) with a calibration accuracy of 5% (Nault et al., 2015). HNO<sub>4</sub> and CH<sub>3</sub>O<sub>2</sub>NO<sub>2</sub> are independently measured with calibration accuracies of 15%, and the CH<sub>3</sub>O<sub>2</sub>NO<sub>2</sub> measurement has an overall uncertainty of 40%, mainly due to uncertainty in the thermal decomposition rate constant (Nault et al., 2015). An independent NO<sub>2</sub> measurement made by chemiluminescence (Pollack et al., 2010) during SEAC<sup>4</sup>RS was biased high compared to the TD-LIF measurement, likely due to interferences from CH<sub>3</sub>O<sub>2</sub>NO<sub>2</sub> and HNO<sub>4</sub> (Travis et al., 2016). The Berkeley TD-LIF NO<sub>2</sub> measurements in the upper troposphere have been used in previous work to interpret NO<sub>x</sub> chemistry (Nault et al., 2016), lightning NO<sub>x</sub> emissions (Nault et al., 2017), and satellite observations of NO<sub>2</sub> columns (Choi et al., 2014; Laughner & Cohen, 2017).

The model-measurement discrepancy in NO/NO<sub>2</sub> partitioning in the upper troposphere has consequences not only for tropospheric chemistry but also for interpreting solar backscatter NO<sub>2</sub> observations from satellites. It is generally assumed that the tropospheric NO<sub>2</sub> column retrieved from satellites is mainly contributed by the boundary layer (Lamsal et al., 2014; Laughner et al., 2016; Martin et al., 2002) and can therefore be related to local NO<sub>x</sub> emissions (Martin et al., 2003). However, the NO<sub>2</sub> vertical profiles from SEAC<sup>4</sup>RS imply a 35–50% contribution of the upper troposphere to the NO<sub>2</sub> tropospheric column observed from satellite (Travis et al., 2016), because sensitivity of backscattered solar radiation to NO<sub>2</sub> increases by a factor of 3 from the surface to the upper troposphere (Martin et al., 2002). Better understanding of this upper tropospheric NO<sub>2</sub> is crucial to the use of satellite data for estimating surface NO<sub>x</sub> emissions.

Previous work starting in the 1990s has found varied levels of agreement between NO/NO<sub>2</sub> ratios observed from aircraft and model photochemical equilibrium computed from local conditions. Early work in the lower stratosphere found models to be too high by 20–30% (Cohen et al., 2000; Del Negro et al., 1999; Jaeglé et al., 1994; Sen et al., 1998). Observed NO/NO<sub>2</sub> ratios in the upper troposphere during the PEM-West A campaign over the tropical Pacific were three times lower than model predictions, which was attributed to NO<sub>2</sub> measurement interferences (Crawford et al., 1996), although Davis et al. (1996) also hypothesized a role of halogen chemistry. Bradshaw et al. (1999) found model agreement with observations to within 30% in the upper troposphere over the tropical Pacific using an improved NO<sub>2</sub> instrument that avoided positive interferences through short inlet residence time. More recent model studies of the upper troposphere have again found an overestimate of observed NO/NO<sub>2</sub> ratios (Travis et al., 2016; Williams et al., 2017) and attributed it to underestimate of peroxy radicals converting NO to NO<sub>2</sub>.

## 2. NO-NO<sub>2</sub> Cycling in the Upper Troposphere During SEAC<sup>4</sup>RS

According to current understanding, the NO/NO<sub>2</sub> ratio in the daytime upper troposphere is determined by rapid chemical cycling through the reactions in Table 1. Here we calculated the mean rates of individual

**Table 1**  
 NO-NO<sub>2</sub> Cycling in the Upper Troposphere During SEAC<sup>4</sup>RS<sup>a</sup>

Reaction	Mean rate (10 <sup>6</sup> molecules · cm <sup>-3</sup> · s <sup>-1</sup> )
Conversion of NO to NO <sub>2</sub>	
R1. NO + O <sub>3</sub> → NO <sub>2</sub> + O <sub>2</sub>	3.42 ± 1.04 <sup>b,d</sup>
R2. NO + HO <sub>2</sub> → NO <sub>2</sub> + OH	0.68 ± 0.23 <sup>b,d,e</sup>
R3. NO + CH <sub>3</sub> O <sub>2</sub> → NO <sub>2</sub> + CH <sub>3</sub> O	0.13 ± 0.04 <sup>b,d,e</sup>
R4. NO + BrO → NO <sub>2</sub> + Br	0.18 ± 0.09 <sup>b,d,f</sup>
R5. NO + IO → NO <sub>2</sub> + I	0.10 ± 0.05 <sup>b,d,f</sup>
R6. NO + ClO → NO <sub>2</sub> + Cl	0.02 ± 0.01 <sup>b,d,f</sup>
Total	4.53 ± 1.46
Conversion of NO <sub>2</sub> to NO	
R7. NO <sub>2</sub> + hν → NO + O	8.20 ± 1.74 <sup>g</sup>

<sup>a</sup>Main reactions cycling NO and NO<sub>2</sub> in the daytime upper troposphere (8–12 km) over the southeast United States. Mean rates are calculated using JPL kinetic data (Burkholder et al., 2015) applied to SEAC<sup>4</sup>RS aircraft observations (NO, NO<sub>2</sub>, O<sub>3</sub>, J<sub>NO2</sub>, temperature, and pressure) over the southeast United States (94.5–76°W, 30–37°N) in August–September 2013 and with radical concentrations (RO<sub>2</sub>, halogens) computed by the GEOS-Chem model along the flight tracks (Sherwen et al., 2016, 2017; Travis et al., 2016). Only reactions with rates above 1 × 10<sup>4</sup> molecules · cm<sup>-3</sup> · s<sup>-1</sup> are listed. Data outside the 9–15 solar time window and in stratospheric air ([O<sub>3</sub>]/[CO] > 1.25 mol mol<sup>-1</sup>) have been excluded. Error standard deviations are calculated by propagation of measurement, rate constant, and GEOS-Chem radical concentration errors (precision). <sup>b</sup>Precision of the NO measurement (4%; Ryerson et al., 2000). <sup>c</sup>Precision of the O<sub>3</sub> measurement (3%; Ryerson et al., 1998). <sup>d</sup>Precision of the kinetic rate constants (30% for NO + O<sub>3</sub>, 15% for NO + HO<sub>2</sub>, NO + CH<sub>3</sub>O<sub>2</sub>, NO + BrO, and NO + ClO, and 20% for NO + IO; Burkholder et al., 2015). <sup>e</sup>Uncertainty in the GEOS-Chem HO<sub>2</sub> concentration (30%) estimated from the H<sub>2</sub>O<sub>2</sub> measurements in SEAC<sup>4</sup>RS (Crouse et al., 2006). The same relative error is assumed for CH<sub>3</sub>O<sub>2</sub>. <sup>f</sup>Uncertainty in the GEOS-Chem BrO, IO, and ClO concentrations (50%; Sherwen et al., 2016). <sup>g</sup>Precision of the NO<sub>2</sub> measurement (5%; Nault et al., 2015), the measured UV-A actinic flux (5%; Shetter et al., 2003), and the NO<sub>2</sub> cross section and quantum yield (20%; Sander et al., 2011).

reactions along the SEAC<sup>4</sup>RS flight tracks over the southeast United States by applying the recommended Jet Propulsion Laboratory (JPL) rate constants (Burkholder et al., 2015) to aircraft measurements of species concentrations (NO, NO<sub>2</sub>, and O<sub>3</sub>), NO<sub>2</sub> photolysis rate constant (J<sub>NO2</sub>), temperature, and pressure, together with peroxy and halogen radical concentrations computed by the GEOS-Chem model (Sherwen et al., 2016, 2017; Travis et al., 2016) along the flight tracks. We exclude data outside the 9–15 hr solar time window and in stratospheric air ([O<sub>3</sub>]/[CO] > 1.25 mol mol<sup>-1</sup>). We focus on the southeast United States because it accounts for most of the SEAC<sup>4</sup>RS flights and represents a relatively homogeneous environment.

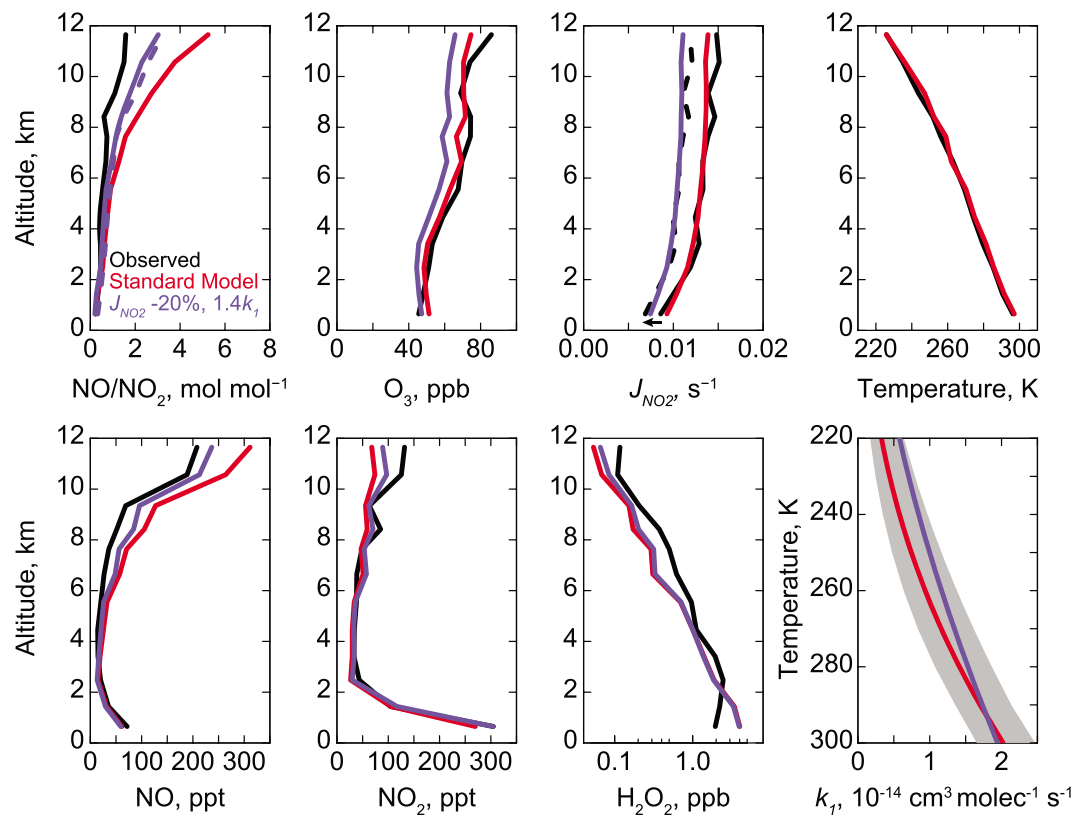
The calculated rates in Table 1 indicate that conversion of NO to NO<sub>2</sub> in the upper troposphere is mainly by reaction with ozone (75%). Reactions with peroxy radicals contribute 18%, and reactions with halogen radicals (BrO, IO, and ClO) contribute 7%. The total calculated rate of conversion of NO to NO<sub>2</sub> has an aggregated uncertainty of 32% and balances only half of the NO<sub>2</sub> photolysis rate, which has an uncertainty of 21%. This represents a significant discrepancy, such that a model using JPL kinetics would overestimate the NO/NO<sub>2</sub> ratio observed in SEAC<sup>4</sup>RS.

Figure 1 shows the median observed vertical profiles of the principal variables relevant to NO/NO<sub>2</sub> cycling, along with the corresponding values simulated by the standard GEOS-Chem model along the aircraft flight tracks as in Travis et al. (2016). The NO/NO<sub>2</sub> ratio in the model is over twice that measured in the upper troposphere above 8 km. The bias is systematic over the frequency distribution of the observations (Figure 2) and also extends to stratospherically influenced air ([O<sub>3</sub>]/[CO] > 1.25 mol mol<sup>-1</sup>), although SEAC<sup>4</sup>RS did not sample the actual stratosphere (maximum ozone concentration was 125 ppb). Travis et al. (2016) attributed the model bias in the NO/NO<sub>2</sub> ratio to an underestimate of peroxy radicals, but that underestimate would have to be a factor of 5 in order to close the budget of Table 1. This is incompatible with the SEAC<sup>4</sup>RS observations for H<sub>2</sub>O<sub>2</sub>, which is produced by self-reaction

of HO<sub>2</sub> and is thus a sensitive proxy of HO<sub>2</sub> concentrations. Observed H<sub>2</sub>O<sub>2</sub> concentrations are 30% higher than GEOS-Chem (Figure 1) but would be grossly overestimated if HO<sub>2</sub> concentrations were increased by a factor of 5. Similarly, simulated BrO concentrations would have to be underestimated by a factor of 20 in order to correct the model bias in the NO/NO<sub>2</sub> ratio. This would be grossly inconsistent with observations (Schmidt et al., 2016; Shah et al., 2016; Sherwen et al., 2016).

We see from Figure 1 that there is no systematic model bias in ozone, temperature, or J<sub>NO2</sub> that would explain an error in the NO/NO<sub>2</sub> ratio. The J<sub>NO2</sub> observations during SEAC<sup>4</sup>RS are from spectrally resolved actinic flux measurements (Shetter et al., 2003), converted to photolysis frequencies using the same temperature-dependent JPL spectroscopic data (absorption cross sections and quantum yields) as in GEOS-Chem. These spectroscopic data are tabulated by JPL as a function of wavelength at 220 and 294 K and are interpolated linearly for intermediate temperatures. About 90% of J<sub>NO2</sub> photolysis is contributed by wavelengths shorter than 398 nm for which the quantum yield is unity. The estimated JPL uncertainty on J<sub>NO2</sub> is 20% with no temperature dependence (Sander et al., 2011), though laboratory studies show better agreement at surface temperatures (Orphal, 2003; Shetter et al., 2003). Observed photolysis frequencies of other relevant species (O<sub>3</sub>, HCHO, H<sub>2</sub>O<sub>2</sub>, HNO<sub>3</sub>, PAN, and CH<sub>3</sub>OOH) also agree with GEOS-Chem values to within 1–15% throughout the troposphere.

One possible explanation for the apparent departure of the NO/NO<sub>2</sub> ratio from photochemical equilibrium would be a positive bias in the NO<sub>2</sub> measurement. This could occur if there was an unrecognized labile reservoir of NO<sub>2</sub> (other than HNO<sub>4</sub> or CH<sub>3</sub>O<sub>2</sub>NO<sub>2</sub>) decomposing in the instrument inlet, or if the correction for HNO<sub>4</sub> or CH<sub>3</sub>O<sub>2</sub>NO<sub>2</sub> was inadequate. We find that that this missing reservoir (likely organic) would need to



**Figure 1.** Median vertical tropospheric profiles of the NO/NO<sub>2</sub> concentration ratio and related quantities on SEAC<sup>4</sup>RS flights (9–15 solar time) during August–September 2013 over the southeast United States (94.5–76°W, 30–37°N). Data from urban plumes ([NO<sub>2</sub>] > 4 ppt), open fire plumes ([CH<sub>3</sub>CN] > 200 ppt), and stratospheric air ([O<sub>3</sub>]/[CO] > 1.25 mol mol<sup>-1</sup>) are excluded. Observations are compared to GEOS-Chem model results sampled along the flight tracks, for the standard model (Travis et al., 2016), and a sensitivity simulation with reduced  $J_{\text{NO}_2}$  and increased low-temperature NO + O<sub>3</sub> rate constant (see bottom right panel). Observed NO<sub>2</sub> is from the Berkeley TD-LIF measurement (Nault et al., 2015). The bottom right panel shows the  $k_1$  (NO + O<sub>3</sub>) rate constant versus temperature from JPL in red with 2- $\sigma$  uncertainty in gray shading (Burkholder et al., 2015), and sensitivity simulation values resulting in 1.4 $k_1$  (purple) in the upper troposphere. The  $J_{\text{NO}_2}$  observations apply JPL spectroscopic data to actinic fluxes measured aboard the aircraft and would be reduced similarly to the model if the spectroscopic data are corrected downward (black dashed line). The dashed purple line in the top left panel shows the NO-NO<sub>2</sub>-O<sub>3</sub> photochemical equilibrium values  $J_{\text{NO}_2}(h\nu)/k_1(T)[\text{O}_3]$  calculated from observed actinic fluxes ( $h\nu$ ), temperature ( $T$ ), and [O<sub>3</sub>] with 1.4 $k_1$  and the 20% reduction in  $J_{\text{NO}_2}$  applied.

be present at a mean concentration of at least 40 ppt in the upper troposphere in order to fit the model NO/NO<sub>2</sub> ratios, assuming 100% decomposition to NO<sub>2</sub> inside the instrument. For comparison, the correction to the NO<sub>2</sub> measurement from the decomposition of CH<sub>3</sub>O<sub>2</sub>NO<sub>2</sub> was 0–23 ppt (0–21% of NO<sub>2</sub> at temperatures less than 240 K) and 0–20 ppt HNO<sub>4</sub> (0–11%) during SEAC<sup>4</sup>RS (Nault et al., 2015). The high-flow pump to minimize the influence from these reservoirs malfunctioned in the first five SEAC<sup>4</sup>RS flights (6–16 August), but these flights were either not over the southeast United States or not in the upper troposphere and are not included in our analysis.

A significant uncertainty in the CH<sub>3</sub>O<sub>2</sub>NO<sub>2</sub> correction is the thermal decomposition rate constant, which has a JPL 1- $\sigma$  uncertainty of 30%. Considering a cabin air temperature of 300 K, an exterior pressure of 230 hPa, and an inlet residence time of 0.23 s, a 30% increase in the CH<sub>3</sub>O<sub>2</sub>NO<sub>2</sub> thermal decomposition rate would double the corresponding correction to the NO<sub>2</sub> measurement from 0–23 to 0–46 ppt. The effect would be at most 23 ppt at the upper end of the range and is not sufficient to correct the NO/NO<sub>2</sub> ratio. GEOS-Chem underestimates CH<sub>3</sub>O<sub>2</sub>NO<sub>2</sub> in the upper troposphere (18 ± 19 ppt modeled, 124 ± 98 ppt observed), reflecting in part the model underestimate of NO<sub>2</sub> but also suggesting missing organic chemistry. A faster thermal decomposition rate for CH<sub>3</sub>O<sub>2</sub>NO<sub>2</sub> would exacerbate the model underestimate.



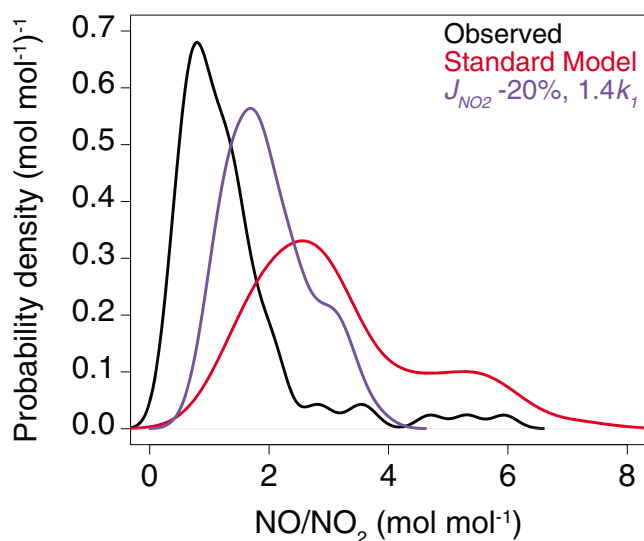


**Figure 2.** Probability density function of the NO/NO<sub>2</sub> concentration ratio under midday conditions (9–15 local time) in the upper troposphere (8–12 km) during SEAC<sup>4</sup>RS in August–September 2013. Observations are compared to the standard GEOS-Chem model and the model with  $J_{\text{NO}_2}$  reduced by 20% and the activation energy for the NO + O<sub>3</sub> reaction increased so that  $k_1$  increases on average by 1.4 in the upper troposphere (purple). The same data criteria as stated for Table 1 are applied.

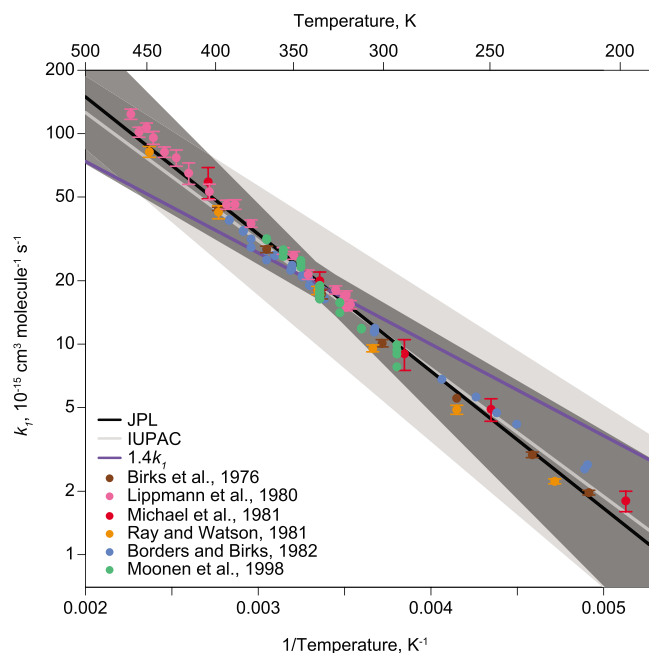


**Figure 3.** Temperature dependence of the NO + O<sub>3</sub> rate constant  $k_1$ . The y axis is a log scale, and the x axis is an inverse scale ( $1/T$ ), so that an Arrhenius dependence plots as a straight line. Recommended rates from JPL (black; Burkholder et al., 2015) and IUPAC (light gray; Atkinson et al., 2004) are shown as solid lines with the 2- $\sigma$  uncertainty in shading. Laboratory measurements used in the JPL and IUPAC recommendations are shown in circles with their respective uncertainties. The sensitivity simulation resulting in  $1.4k_1$  in the upper troposphere (230–250 K) is shown as the purple line.

Previous work has postulated missing organic chemistry in the upper troposphere to explain observations of volatile organic compounds (VOCs) including methanol (Jacob et al., 2005), acetaldehyde (Millet et al., 2010), and glyoxal (Volkamer et al., 2015). Aumont et al. (2005) and Mouchel-Vallon et al. (2013) showed how explicit VOC mechanisms produce a cascade of oxidation products globally that are not tracked in models. Bradshaw et al. (1999) did not need to invoke an unknown NO<sub>x</sub> reservoir to reconcile their model with observations over the tropical Pacific, but the southeast United States may be a more propitious environment for VOC oxidation products to be lifted to the upper troposphere by deep convection (Li et al., 2005).

An alternative explanation for the apparent NO/NO<sub>2</sub> departure from photochemical equilibrium would be error in the kinetic data used to compute that equilibrium. Figure 3 shows the International Union of Pure and Applied Chemistry (IUPAC) and JPL recommendations for the temperature dependence of the NO + O<sub>3</sub> rate constant  $k_1$ , along with the individual laboratory data that went into these recommendations. IUPAC recommends  $k_1 = 2.07 \times 10^{-12} \exp[-1400/T]$  cm<sup>3</sup> · molecule<sup>-1</sup> · s<sup>-1</sup> with a 1- $\sigma$  uncertainty of  $\pm 200$  K for  $E/R$  and a 1- $\sigma$  uncertainty of 8% for  $k_1$  at 298 K (Atkinson et al., 2004). JPL recommends  $k_1 = 3.00 \times 10^{-12} \exp[-1500/T]$ , again with 1- $\sigma$  uncertainty of  $\pm 200$  K for  $E/R$  and a 1- $\sigma$  uncertainty of 10% for  $k_1$  at 298 K. The IUPAC and JPL rate expressions agree to within 4% over the 220–300 K temperature range. For a typical upper tropospheric temperature of 220–240 K the implied 1- $\sigma$  uncertainty for the JPL rate is 30–40%. However, several studies have suggested a departure from Arrhenius behavior at low temperatures (Figure 3; Birks et al., 1976; Borders & Birks, 1982; Cohen et al., 2000; Michael et al., 1981).

The purple curves in Figures 1 and 2 show the effects in the GEOS-Chem simulation of decreasing  $J_{\text{NO}_2}$  by 20%, and decreasing the activation energy for  $k_1$  by 400 K ( $2\sigma$ ) relative to the JPL recommendation so that  $k_1$  increases by a factor 1.4 on average in the upper troposphere, while remaining at the JPL recommended value at 298 K through adjustment of the preexponential factor. The resulting NO/NO<sub>2</sub> ratio in the upper troposphere decreases by 40% from the standard simulation, and Figure 2 shows that the variance in the modeled NO/NO<sub>2</sub> ratio decreases by half, becoming more consistent with the observations. One could match the observations if there was in addition a 15 ppt positive bias in the NO<sub>2</sub> measurement due to an unaccounted labile NO<sub>x</sub> reservoir.

We examined whether the variability of the observed NO/NO<sub>2</sub> ratio in the SEAC<sup>4</sup>RS data set could test the above corrections. For this purpose we used 10-min observations of the ratio along the flight tracks at 8–12 km altitude and correlated them to the local values of the photoequilibrium constant  $J_{\text{NO}_2}(h\nu)/k_1(T)[\text{O}_3]$  for NO-NO<sub>2</sub>-O<sub>3</sub> cycling where the UV actinic fluxes ( $h\nu$ ), temperatures ( $T$ ), and [O<sub>3</sub>] are taken from the observations. Results are shown in Figure 4. When using JPL values for  $J_{\text{NO}_2}(h\nu)$  and  $k_1(T)$ , we find a significant ( $p < 0.01$ ) correlation coefficient  $r = 0.37$  and a reduced-major-axis regression slope  $S = 4.0$ . The relatively low correlation coefficient can be attributed to noise and high-frequency variability in the observations. Reducing  $J_{\text{NO}_2}$  by 20% and increasing the low-temperature  $k_1$  as described above improves the slope ( $S = 2.3$ ) while not affecting the correlation coefficient

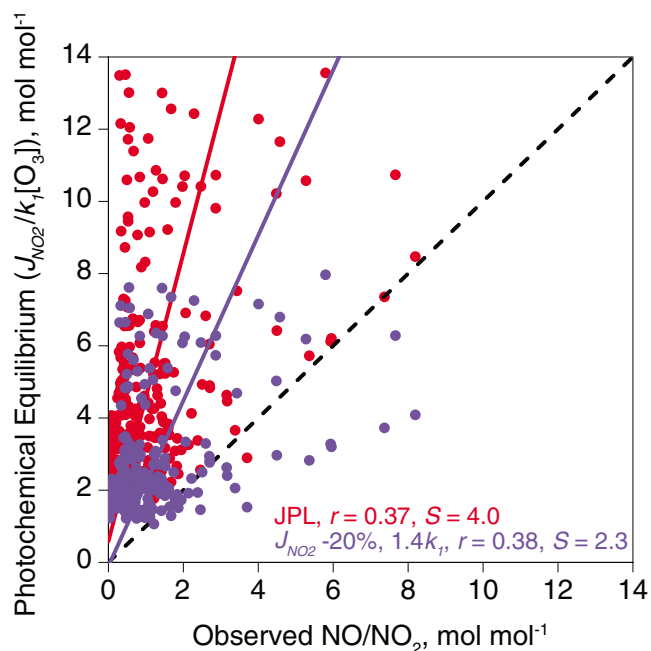


**Figure 4.** Correlation of the observed NO/NO<sub>2</sub> concentration ratio with the local photochemical equilibrium constant  $J_{\text{NO}_2}(h\nu)/k_1(T)[\text{O}_3]$  under midday conditions (9–15 local time) in the upper troposphere (8–12 km) during SEAC<sup>4</sup>RS in August–September 2013. Data are 10-min averages along the aircraft flight tracks. The photochemical equilibrium constant is calculated from local aircraft measurements of actinic fluxes ( $h\nu$ ), temperature ( $T$ ), and ozone concentrations. Calculations using the JPL recommendations for  $J_{\text{NO}_2}(h\nu)$  and  $k_1(T)$  (in red) are compared to calculations reducing  $J_{\text{NO}_2}$  by 20% and increasing  $k_1$  on average by 1.4 in the upper troposphere (purple). The solid lines show reduced major axis regressions and the 1:1 line is dashed. Correlation coefficients ( $r$ ) and regression slopes ( $S$ ) are given inset.

2017; Ridley et al., 2017; Vuilleumier et al., 1997). When the low-temperature NO + O<sub>3</sub> reaction rate constant ( $1.4k_1$ ) and NO<sub>2</sub> photolysis frequency ( $J_{\text{NO}_2} - 20\%$ ) are adjusted in GEOS-Chem within these uncertainties to improve the simulation of the NO/NO<sub>2</sub> ratio in the SEAC<sup>4</sup>RS upper tropospheric data, we find that simulated ozone decreases by 7 ppb at 8–12 km altitude. This degrades the previously successful simulation of upper tropospheric ozone in the standard model (Travis et al., 2016); however, that simulation overestimated the NO concentration (Figure 1).

Improved understanding of the contribution of the upper troposphere to the tropospheric NO<sub>2</sub> column also has implications for retrieving and interpreting NO<sub>2</sub> observations from satellites. Spectral fitting of the satellite data in and around the NO<sub>2</sub> absorption bands measures the slant column of NO<sub>2</sub> along the light path. Conversion of this slant column to the actual vertical tropospheric column requires removal of the stratospheric contribution, followed by division by an air mass factor (AMF) dependent on the vertical distribution of tropospheric NO<sub>2</sub> (Martin et al., 2002). The National Aeronautics and Space Administration (NASA) operational retrieval for the OMI satellite instrument (Krotkov et al., 2017) assumes NO<sub>2</sub> vertical profiles from the GMI model (Lamsal et al., 2014) that greatly underestimate NO<sub>2</sub> concentrations in the upper troposphere as observed by SEAC<sup>4</sup>RS. The mean AMF over the southeast United States in August–September 2013 is 1.28 using vertical distributions from the NASA operational retrieval but 1.67 when using the median observed profile in Figure 1. This implies that the OMI operational retrieval for NO<sub>2</sub> may be 30% too high. Laughner and Cohen (2017) show that inclusion of lightning NO<sub>x</sub> in the upper troposphere to match DC3 observations of NO<sub>2</sub> increases the OMI AMF by 34% for summertime, further demonstrating the importance of accurately modeling and measuring NO<sub>x</sub> in the upper troposphere for the interpretation of satellite NO<sub>2</sub> measurements.

( $r = 0.38$ ). Excluding the 15% of the data with  $[\text{O}_3] < 40$  ppb increases the correlation coefficient to  $r = 0.48$ – $0.49$ . Those conditions were associated with particularly high  $J_{\text{NO}_2}$  (reflecting clouds below) and enhancements in CO and HCHO indicative of recent convective influence (Barth et al., 2015; Fried et al., 2016; Snow et al., 2007).

### 3. Implications

The apparent departure of the NO/NO<sub>2</sub> concentration ratio from photochemical equilibrium in upper tropospheric observations cannot be explained by missing radicals converting NO to NO<sub>2</sub>, as proposed in previous work, because the required radical concentrations would be far in excess of observational constraints. It must be due either to an unaccounted labile NO<sub>x</sub> reservoir acting as positive interference on the NO<sub>2</sub> measurement or to significant errors in the kinetic data for NO–NO<sub>2</sub>–O<sub>3</sub> photochemical cycling at low temperatures. Either of these possibilities have important implications for upper tropospheric chemistry.

The NO<sub>2</sub> measurement specifically excludes interferences from HNO<sub>4</sub> and CH<sub>3</sub>O<sub>2</sub>NO<sub>2</sub>, but other labile NO<sub>x</sub> reservoirs could potentially be measured as NO<sub>2</sub> following thermal decomposition in the instrument. The presence of such a reservoir at a concentration of 40 ppt, as needed to explain the observed NO/NO<sub>2</sub> ratios, would increase the effective lifetime of NO<sub>x</sub> by 20% under the SEAC<sup>4</sup>RS conditions. More importantly, it would likely imply organic chemistry missing from the models, as also suggested by observations of acetaldehyde and glyoxal in the upper troposphere (Millet et al., 2010; Volkamer et al., 2015) and by the large model underestimate of CH<sub>3</sub>O<sub>2</sub>NO<sub>2</sub> in SEAC<sup>4</sup>RS.

The rate constants  $J_{\text{NO}_2}$  and  $k_1$  involved in NO–NO<sub>2</sub>–O<sub>3</sub> photochemical cycling have relatively small uncertainties in kinetic assessments, and even then are found to be major sources of uncertainty in model simulations of tropospheric oxidants (Bergin et al., 1999; Newsome & Evans,

In conclusion, models significantly overestimate recent observations of the NO/NO<sub>2</sub> ratio in the upper troposphere. This cannot be easily explained by known labile NO<sub>x</sub> reservoirs (HNO<sub>4</sub> and CH<sub>3</sub>O<sub>2</sub>NO<sub>2</sub>) interfering with the NO<sub>2</sub> measurement. It implies either error in current recommendations for NO-NO<sub>2</sub>-O<sub>3</sub> cycling kinetics or the presence of a missing labile NO<sub>x</sub> reservoir, likely organic. Either explanation would have important implications for our understanding of tropospheric oxidants and/or the interpretation of satellite NO<sub>2</sub> measurements.

#### Acknowledgments

We thank Tom Ryerson for his measurements of NO and O<sub>3</sub> from the NOAA NO<sub>y</sub>O<sub>3</sub> instrument. This work was supported by the NASA Earth Science Division and USEPA grant 83587201. Its contents are solely the responsibility of the grantee and do not necessarily represent the official views of the USEPA. Further, USEPA does not endorse the purchase of any commercial products or services mentioned in the publication. SEAC<sup>4</sup>RS airborne measurements are available from the NASA LaRC Airborne Science Data for Atmospheric Composition (<http://www-air.larc.nasa.gov/cgi-bin/ArcView/seac4rs>). OMI NO<sub>2</sub> observations are available from the NASA Goddard Earth Sciences Data and Information Services Center ([https://aura.gesdisc.eosdis.nasa.gov/data/Aura\\_OMI\\_Level2/OMNO2.003/](https://aura.gesdisc.eosdis.nasa.gov/data/Aura_OMI_Level2/OMNO2.003/)).

#### References

- Atkinson, R., Baulch, D. L., Cox, R. A., Crowley, J. N., Hampson, R. F., Hynes, R. G., et al. (2004). IUPAC task group on atmospheric chemical kinetic data evaluation. *Atmospheric Chemistry and Physics*, 4(6), 1461–1738. <https://doi.org/10.5194/acp-4-1461-2004>
- Aumont, B., Szopa, S., & Madronich, S. (2005). Modelling the evolution of organic carbon during its gas-phase tropospheric oxidation: Development of an explicit model based on a self generating approach. *Atmospheric Chemistry and Physics*, 5(9), 2497–2517. <https://doi.org/10.5194/acp-5-2497-2005>
- Barth, M. C., Cantrell, C. A., Brune, W. H., Rutledge, S. A., Crawford, J. H., Huntrieser, H., et al. (2015). The Deep Convective Clouds and Chemistry (DC3) field campaign. *Bulletin of the American Meteorological Society*, 96(8), 1281–1309. <https://doi.org/10.1175/bams-d-13-00290.1>
- Bergin, M. S., Noblet, G. S., Petrini, K., Dhieux, J. R., Milford, J. B., & Harley, R. A. (1999). Formal uncertainty analysis of a Lagrangian photochemical air pollution model. *Environmental Science & Technology*, 33(7), 1116–1126. <https://doi.org/10.1021/es980749y>
- Bertram, T. H., Perring, A. E., Wooldridge, P. J., Crounse, J. D., Kwan, A. J., Wennberg, P. O., et al. (2007). Direct measurements of the convective recycling of the upper troposphere. *Science*, 315(5813), 816–820. <https://doi.org/10.1126/science.1134548>
- Birks, J. W., Shoemaker, B., Leck, T. J., & Hinton, D. M. (1976). Studies of reactions of importance in the stratosphere. 1. Reaction of nitric oxide with ozone. *Journal of Chemical Physics*, 65(12), 5181–5185. <https://doi.org/10.1063/1.433059>
- Borders, R. A., & Birks, J. W. (1982). High-precision measurements of activation energies over small temperature intervals: Curvature in the Arrhenius plot for the reaction NO + O<sub>3</sub> → NO<sub>2</sub> + O<sub>2</sub>. *Journal of Physical Chemistry*, 86(17), 3295–3302. <https://doi.org/10.1021/j100214a007>
- Bradshaw, J., Davis, D., Crawford, J., Chen, G., Shetter, R., Muller, M., et al. (1999). Photofragmentation two-photon laser-induced fluorescence detection of NO<sub>2</sub> and NO: Comparison of measurements with model results based on airborne observations during PEM-Tropics A. *Geophysical Research Letters*, 26, 471–474. <https://doi.org/10.1029/1999GL900015>
- Browne, E. C., Perring, A. E., Wooldridge, P. J., Apel, E., Hall, S. R., Huey, L. G., et al. (2011). Global and regional effects of the photochemistry of CH<sub>3</sub>O<sub>2</sub>NO<sub>2</sub>: Evidence from ARCTAS. *Atmospheric Chemistry and Physics*, 11(9), 4209–4219. <https://doi.org/10.5194/acp-11-4209-2011>
- Burkholder, J. B., Sander, S. P., Abbatt, J., Barker, J. R., Huie, R. E., Kolb, C. E., et al. (2015). Chemical kinetics and photochemical data for use in atmospheric studies, Evaluation No. 18. <http://jpldataeval.jpl.nasa.gov/>
- Choi, S., Joiner, J., Choi, Y., Duncan, B. N., Vasilkov, A., Krotkov, N., & Bucsel, E. (2014). First estimates of global free-tropospheric NO<sub>2</sub> abundances derived using a cloud-slicing technique applied to satellite observations from the Aura Ozone Monitoring Instrument (OMI). *Atmospheric Chemistry and Physics*, 14(19), 10,565–10,588. <https://doi.org/10.5194/acp-14-10565-2014>
- Cohen, R. C., Perkins, K. K., Koch, L. C., Stimpfle, R. M., Wennberg, P. O., Hanisco, T. F., et al. (2000). Quantitative constraints on the atmospheric chemistry of nitrogen oxides: An analysis along chemical coordinates. *Journal of Geophysical Research*, 105, 24,283–24,304. <https://doi.org/10.1029/2000JD900290>
- Crawford, J., Davis, D., Chen, G., Bradshaw, J., Sandholm, S., Gregory, G., et al. (1996). Photostationary state analysis of the NO<sub>2</sub>-NO system based on airborne observations from the western and central North Pacific. *Journal of Geophysical Research*, 101, 2053–2072. <https://doi.org/10.1029/95JD02201>
- Crounse, J. D., McKinney, K. A., Kwan, A. J., & Wennberg, P. O. (2006). Measurement of gas-phase hydroperoxides by chemical ionization mass spectrometry. *Analytical Chemistry*, 78(19), 6726–6732. <https://doi.org/10.1021/ac0604235>
- Davis, D., Crawford, J., Liu, S., McKeen, S., Bandy, A., Thornton, D., et al. (1996). Potential impact of iodine on tropospheric levels of ozone and other critical oxidants. *Journal of Geophysical Research*, 101, 2135–2147. <https://doi.org/10.1029/95JD02272>
- Day, D. A., Wooldridge, P. J., Dillon, M. B., Thornton, J. A., & Cohen, R. C. (2002). A thermal dissociation laser-induced fluorescence instrument for in situ detection of NO<sub>2</sub>, peroxy nitrates, alkyl nitrates, and HNO<sub>3</sub>. *Journal of Geophysical Research*, 107(D6), 4046. <https://doi.org/10.1029/2001JD000779>
- Del Negro, L. A., Fahey, D. W., Gao, R. S., Donnelly, S. G., Keim, E. R., Neuman, J. A., et al. (1999). Comparison of modeled and observed values of NO<sub>2</sub> and J<sub>NO2</sub> during the Photochemistry of Ozone Loss in the Arctic Region in Summer (POLARIS) mission. *Journal of Geophysical Research*, 104, 26,687–26,703. <https://doi.org/10.1029/1999JD900246>
- Fried, A., Barth, M. C., Bela, M., Weibring, P., Richter, D., Walega, J., et al. (2016). Convective transport of formaldehyde to the upper troposphere and lower stratosphere and associated scavenging in thunderstorms over the central United States during the 2012DC3 study. *Journal of Geophysical Research: Atmospheres*, 121, 7430–7460. <https://doi.org/10.1002/2015JD024477>
- Hudman, R. C., Jacob, D. J., Turquety, S., Leibensperger, E. M., Murray, L. T., Wu, S., et al. (2007). Surface and lightning sources of nitrogen oxides over the United States: Magnitudes, chemical evolution, and outflow. *Journal of Geophysical Research*, 112, D12S05. <https://doi.org/10.1029/2006JD007912>
- Huntrieser, H., Feigl, C., Schlager, H., Schroder, F., Gerbig, C., van Velthoven, P., et al. (2002). Airborne measurements of NO<sub>x</sub>, tracer species, and small particles during the European lightning nitrogen oxides experiment. *Journal of Geophysical Research*, 107(D11), 4113. <https://doi.org/10.1029/2000JD000209>
- Jacob, D. J., Field, B. D., Li, Q. B., Blake, D. R., de Gouw, J., Warneke, C., et al. (2005). Global budget of methanol: Constraints from atmospheric observations. *Journal of Geophysical Research*, 110, D08303. <https://doi.org/10.1029/2004JD005172>
- Jaeglé, L., Webster, C. R., May, R. D., Fahey, D. W., Woodbridge, E. L., Keim, E. R., et al. (1994). In-situ measurements of the NO<sub>2</sub>/NO ratio for testing atmospheric photochemical models. *Geophysical Research Letters*, 21, 2555–2558. <https://doi.org/10.1029/94GL02717>
- Krotkov, N. A., Lamsal, L. N., Celarier, E. A., Swartz, W. H., Marchenko, S. V., Bucsel, E. J., et al. (2017). The version 3 OMI NO<sub>2</sub> standard product. *Atmospheric Measurement Techniques*, 10(9), 3133–3149. <https://doi.org/10.5194/amt-10-3133-2017>
- Lamsal, L. N., Krotkov, N. A., Celarier, E. A., Swartz, W. H., Pickering, K. E., Bucsel, E. J., et al. (2014). Evaluation of OMI operational standard NO<sub>2</sub> column retrievals using in situ and surface-based NO<sub>2</sub> observations. *Atmospheric Chemistry and Physics*, 14(21), 11,587–11,609. <https://doi.org/10.5194/acp-14-11587-2014>

- Laughner, J. L., & Cohen, R. C. (2017). Quantification of the effect of modeled lightning NO<sub>2</sub> on UV-visible air mass factors. *Atmospheric Measurement Techniques*, 10(11), 4403–4419. <https://doi.org/10.5194/amt-10-4403-2017>
- Laughner, J. L., Zare, A., & Cohen, R. C. (2016). Effects of daily meteorology on the interpretation of space-based remote sensing of NO<sub>2</sub>. *Atmospheric Chemistry and Physics*, 16(23), 15,247–15,264. <https://doi.org/10.5194/acp-16-15247-2016>
- Li, Q. B., Jacob, D. J., Park, R., Wang, Y. X., Heald, C. L., Hudman, R., et al. (2005). North American pollution outflow and the trapping of convectively lifted pollution by upper-level anticyclone. *Journal of Geophysical Research*, 110, D10301. <https://doi.org/10.1029/2004JD005039>
- Lippmann, H. H., Jesser, B., & Schurath, U. (1980). The rate constant of NO + O<sub>3</sub> → NO<sub>2</sub> + O<sub>2</sub> in the temperature range of 283–443 K. *International Journal of Chemical Kinetics*, 12(8), 547–554. <https://doi.org/10.1002/kin.550120805>
- Martin, R. V., Chance, K., Jacob, D. J., Kurosu, T. P., Spurr, R. J. D., Bucsele, E., et al. (2002). An improved retrieval of tropospheric nitrogen dioxide from GOME. *Journal of Geophysical Research*, 107(D20), 4437. <https://doi.org/10.1029/2001JD001027>
- Martin, R. V., Jacob, D. J., Chance, K., Kurosu, T. P., Palmer, P. I., & Evans, M. J. (2003). Global inventory of nitrogen oxide emissions constrained by space-based observations of NO<sub>2</sub> columns. *Journal of Geophysical Research*, 108(D17), 4537. <https://doi.org/10.1029/2003JD003453>
- Michael, J. V., Allen, J. E., & Brobst, W. D. (1981). Temperature dependence of the NO + O<sub>3</sub> reaction rate from 195 to 369 K. *Journal of Physical Chemistry*, 85(26), 4109–4117. <https://doi.org/10.1021/j150626a032>
- Millet, D. B., Guenther, A., Siegel, D. A., Nelson, N. B., Singh, H. B., de Gouw, J. A., et al. (2010). Global atmospheric budget of acetaldehyde: 3-D model analysis and constraints from in-situ and satellite observations. *Atmospheric Chemistry and Physics*, 10(7), 3405–3425. <https://doi.org/10.5194/acp-10-3405-2010>
- Moonen, P. C., Cape, J. N., Storeton-West, R. L., & McCOLM, R. (1998). Measurement of the NO + O<sub>3</sub> reaction rate at atmospheric pressure using realistic mixing ratios. *Journal of Atmospheric Chemistry*, 29(3), 299–314. <https://doi.org/10.1023/a:1005936016311>
- Mouchel-Vallon, C., Brauer, P., Camredon, M., Valorso, R., Madronich, S., Herrmann, H., & Aumont, B. (2013). Explicit modeling of volatile organic compounds partitioning in the atmospheric aqueous phase. *Atmospheric Chemistry and Physics*, 13(2), 1023–1037. <https://doi.org/10.5194/acp-13-1023-2013>
- Murphy, J. G., Thornton, J. A., Wooldridge, P. J., Day, D. A., Rosen, R. S., Cantrell, C., et al. (2004). Measurements of the sum of HO<sub>2</sub>NO<sub>2</sub> and CH<sub>3</sub>O<sub>2</sub>NO<sub>2</sub> in the remote troposphere. *Atmospheric Chemistry and Physics*, 4(2), 377–384. <https://doi.org/10.5194/acp-4-377-2004>
- Murray, L. T., Logan, J. A., & Jacob, D. J. (2013). Interannual variability in tropical tropospheric ozone and OH: The role of lightning. *Journal of Geophysical Research: Atmospheres*, 118, 11,468–11,480. <https://doi.org/10.1002/jgrd.50857>
- Nault, B. A., Garland, C., Pusede, S. E., Wooldridge, P. J., Ullmann, K., Hall, S. R., & Cohen, R. C. (2015). Measurements of CH<sub>3</sub>O<sub>2</sub>NO<sub>2</sub> in the upper troposphere. *Atmospheric Measurement Techniques*, 8(2), 987–997. <https://doi.org/10.5194/amt-8-987-2015>
- Nault, B. A., Garland, C., Wooldridge, P. J., Brune, W. H., Campuzano-Jost, P., Crouse, J. D., et al. (2016). Observational constraints on the oxidation of NO<sub>x</sub> in the upper troposphere. *Journal of Physical Chemistry A*, 120(9), 1468–1478. <https://doi.org/10.1021/acs.jpca.5b07824>
- Nault, B. A., Laughner, J. L., Wooldridge, P. J., Crouse, J. D., Dibb, J., Diskin, G., et al. (2017). Lightning NO<sub>x</sub> emissions: Reconciling measured and modeled estimates with updated NO<sub>x</sub> chemistry. *Geophysical Research Letters*, 44, 9479–9488. <https://doi.org/10.1002/2017GL074436>
- Newsome, B., & Evans, M. (2017). Impact of uncertainties in inorganic chemical rate constants on tropospheric composition and ozone radiative forcing. *Atmospheric Chemistry and Physics*, 17(23), 14,333–14,352. <https://doi.org/10.5194/acp-17-14333-2017>
- Orphal, J. (2003). A critical review of the absorption cross-sections of O-3 and NO<sub>2</sub> in the ultraviolet and visible. *Journal of Photochemistry and Photobiology A-Chemistry*, 157(2–3), 185–209. [https://doi.org/10.1016/s1010-6030\(03\)00061-3](https://doi.org/10.1016/s1010-6030(03)00061-3)
- Pickering, K. E., Wang, Y. S., Tao, W. K., Price, C., & Muller, J. F. (1998). Vertical distributions of lightning NO<sub>x</sub> for use in regional and global chemical transport models. *Journal of Geophysical Research*, 103, 31,203–31,216. <https://doi.org/10.1029/98JD02651>
- Pollack, I. B., Lerner, B. M., & Ryerson, T. B. (2010). Evaluation of ultraviolet light-emitting diodes for detection of atmospheric NO<sub>2</sub> by photolysis-chemiluminescence. *Journal of Atmospheric Chemistry*, 65(2–3), 111–125. <https://doi.org/10.1007/s10874-011-9184-3>
- Ray, G. W., & Watson, R. T. (1981). Kinetics of the reaction NO + O<sub>3</sub> → NO<sub>2</sub> + O<sub>2</sub> from 212 to 422 K. *The Journal of Physical Chemistry*, 85(12), 1673–1676. <https://doi.org/10.1021/j150612a015>
- Reed, C., Evans, M. J., Di Carlo, P., Lee, J. D., & Carpenter, L. J. (2016). Interferences in photolytic NO<sub>2</sub> measurements: Explanation for an apparent missing oxidant? *Atmospheric Chemistry and Physics*, 16(7), 4707–4724. <https://doi.org/10.5194/acp-16-4707-2016>
- Ridley, D., Cain, M., Methven, J., & Arnold, S. (2017). Sensitivity of tropospheric ozone to chemical kinetic uncertainties in air masses influenced by anthropogenic and biomass burning emissions. *Geophysical Research Letters*, 44, 7472–7481. <https://doi.org/10.1002/2017GL073802>
- Ryerson, T. B., Buhr, M. P., Frost, G. J., Goldan, P. D., Holloway, J. S., Hubler, G., et al. (1998). Emissions lifetimes and ozone formation in power plant plumes. *Journal of Geophysical Research*, 103, 22,569–22,583. <https://doi.org/10.1029/98JD01620>
- Ryerson, T. B., Williams, E. J., & Fehsenfeld, F. C. (2000). An efficient photolysis system for fast-response NO<sub>2</sub> measurements. *Journal of Geophysical Research*, 105, 26,447–26,461. <https://doi.org/10.1029/2000JD900389>
- Sander, S. P., Abbatt, J., Barker, J. R., Burkholder, J. B., Friedl, R. R., Huie, G. D. M., et al. (2011). Chemical kinetics and photochemical data for use in atmospheric studies, Evaluation No. 17.
- Schmidt, J. A., Jacob, D. J., Horowitz, H. M., Hu, L., Sherwen, T., Evans, M. J., et al. (2016). Modeling the observed tropospheric BrO background: Importance of multiphase chemistry and implications for ozone, OH, and mercury. *Journal of Geophysical Research: Atmospheres*, 121, 11,819–11,835. <https://doi.org/10.1002/2015JD024229>
- Sen, B., Toon, G. C., Osterman, G. B., Blavier, J. F., Margitan, J. J., Salawitch, R. J., & Yue, G. K. (1998). Measurements of reactive nitrogen in the stratosphere. *Journal of Geophysical Research*, 103, 3571–3585. <https://doi.org/10.1029/97JD02468>
- Shah, V., Jaegle, L., Gratz, L. E., Ambrose, J. L., Jaffe, D. A., Selin, N. E., et al. (2016). Origin of oxidized mercury in the summertime free troposphere over the southeastern US. *Atmospheric Chemistry and Physics*, 16(3), 1511–1530. <https://doi.org/10.5194/acp-16-1511-2016>
- Sherwen, T., Evans, M. J., Sommariva, R., Hollis, L. D. J., Ball, S. M., Monks, P. S., et al. (2017). Effects of halogens on European air-quality. *Faraday Discussions*, 200, 75–100. <https://doi.org/10.1039/c7fd00026j>
- Sherwen, T., Schmidt, J. A., Evans, M. J., Carpenter, L. J., Grossmann, K., Eastham, S. D., et al. (2016). Global impacts of tropospheric halogens (Cl, Br, I) on oxidants and composition in GEOS-Chem. *Atmospheric Chemistry and Physics*, 16(18), 12,239–12,2271. <https://doi.org/10.5194/acp-16-12239-2016>
- Shetter, R. E., Junkermann, W., Swartz, W. H., Frost, G. J., Crawford, J. H., Lefer, B. L., et al. (2003). Photolysis frequency of NO<sub>2</sub>: Measurement and modeling during the International Photolysis Frequency Measurement and Modeling Intercomparison (IPMMI). *Journal of Geophysical Research*, 108(D16), 8544. <https://doi.org/10.1029/2002JD002932>
- Snow, J. A., Heikes, B. G., Shen, H. W., O'Sullivan, D. W., Fried, A., & Walega, J. (2007). Hydrogen peroxide, methyl hydroperoxide, and formaldehyde over North America and the North Atlantic. *Journal of Geophysical Research*, 112, D12807. <https://doi.org/10.1029/2006JD007746>



- Thornton, J. A., Wooldridge, P. J., & Cohen, R. C. (2000). Atmospheric NO<sub>2</sub>: In situ laser-induced fluorescence detection at parts per trillion mixing ratios. *Analytical Chemistry*, 72(3), 528–539. <https://doi.org/10.1021/ac9908905>
- Travis, K. R., Jacob, D. J., Fisher, J. A., Kim, P. S., Marais, E. A., Zhu, L., et al. (2016). Why do models overestimate surface ozone in the Southeast United States? *Atmospheric Chemistry and Physics*, 16(21), 13,561–13,577. <https://doi.org/10.5194/acp-16-13561-2016>
- Volkamer, R., Baidar, S., Campos, T. L., Coburn, S., DiGangi, J. P., Dix, B., et al. (2015). Aircraft measurements of BrO, IO, glyoxal, NO<sub>2</sub>, H<sub>2</sub>O, O-2-O-2 and aerosol extinction profiles in the tropics: Comparison with aircraft-/ship-based in situ and lidar measurements. *Atmospheric Measurement Techniques*, 8(5), 2121–2148. <https://doi.org/10.5194/amt-8-2121-2015>
- Vuilleumier, L., Harley, R. A., & Brown, N. J. (1997). First- and second-order sensitivity analysis of a photochemically reactive system (a Green's function approach). *Environmental Science & Technology*, 31(4), 1206–1217. <https://doi.org/10.1021/es960727g>
- Wild, O., Prather, M. J., & Akimoto, H. (2001). Indirect long-term global radiative cooling from NO<sub>x</sub> emissions. *Geophysical Research Letters*, 28, 1719–1722. <https://doi.org/10.1029/2000GL012573>
- Williams, J. E., Boersma, K. F., Le Sager, P., & Verstraeten, W. W. (2017). The high-resolution version of TM5-MP for optimized satellite retrievals: Description and validation. *Geoscientific Model Development*, 10(2), 721–750. <https://doi.org/10.5194/gmd-10-721-2017>
- Wooldridge, P. J., Perring, A. E., Bertram, T. H., Flocke, F. M., Roberts, J. M., Singh, H. B., et al. (2010). Total peroxy nitrates (sigma PNs) in the atmosphere: The thermal dissociation-laser induced fluorescence (TD-LIF) technique and comparisons to speciated PAN measurements. *Atmospheric Measurement Techniques*, 3(3), 593–607. <https://doi.org/10.5194/amt-3-593-2010>